Ecological Monographs, 0(0), 2021, e01489

Local endemism and ecological generalism in the assembly of root-colonizing fungi

Jose G. Maciá-Vicente [1,2,4] and Flavius Popa [3]

[1]*Institute of Ecology, Evolution and Diversity, Goethe University Frankfurt, Max-von-Laue-Str. 13, Frankfurt am Main 60438 Germany*
[2]*Plant Ecology and Nature Conservation, Wageningen University & Research, PO Box 47, 6700 AA Wageningen, The Netherlands*
[3]*Department of Ecosystem Monitoring, Research & Conservation, Black Forest National Park, Kniebisstraße 67, 77740 Bad Peterstal-Griesbach, Germany*

Citation: Maciá-Vicente, J. G., and F. Popa. 2021. Local endemism and ecological generalism in the assembly of root-colonizing fungi. Ecological Monographs 00(00):e01489. 10.1002/ecm.1489

Abstract. Root-colonizing fungi form species-rich assemblages with key functions in principal ecosystem processes, making them prospectively important players in conservation and applied ecology. Harnessing the processes and services they drive requires a better understanding of their patterns of diversity and community structure, and how these link to function. Here, we search for possible adaptations to contrasting environmental and host conditions, indicative of participation in habitat-specific processes. We surveyed heathland and grassland habitats across a latitudinal gradient in Western Europe, using a spatially explicit design to assess community variation at scales from centimeters, to thousands of kilometers. Root-associated fungi assemble into strongly site-specific communities irrespective of habitat type, shaped by environmental factors and spatial distance operating at different scales, but also by a high level of endemism, likely to be determined by local stochastic processes such as drift and dispersal limitation at short distances. Despite the high site specificity in communities, they are dominated everywhere by a core set of lineages with little preferences toward habitat conditions or host phylogeny. Our results suggest a convergent evolution across phylogenetically distant lineages toward the root-colonizing habit, and a functional redundancy in strategies for habitat colonization and host interaction. Further efforts are needed to integrate functional trait composition in future community ecology studies of root-colonizing fungi.

Key words: *biogeography; endemism; fungi; grasslands; heathlands; mycorrhizas; roots.*

Introduction

Plant roots provide niches for rich assemblages of fungi that play key functions in ecosystem productivity, nutrient cycling, and soil formation. Root and rhizosphere-colonizing fungi are directly responsible for the mineralization of soil organic matter that renders nutrients available to plants, for the massive storage of soil nutrients, and for their transfer to and between plants (Smith and Read 1997, van der Heijden et al. 2015, Klein et al. 2016, Tedersoo et al. 2020*b*). They also confer plant tolerance against environmental stressors (Van der Heijden et al. 1998), or act as parasites and pathogens with important roles in controlling plant diversity and productivity (Ruijven et al. 2020). Considering the effects of fungal associations on plant traits and productivity may enhance predictions of ecosystem dynamics and biosphere impacts of global climate change (Terrer et al. 2016), as well as enable the harnessing of desirable microbial processes in agriculture (Bender et al. 2016). All of this, however, requires a better knowledge of the large-scale diversity and functions of root-associated fungi.

The variation in structure of root-associated fungal communities over broad geographic scales and environmental gradients has been addressed (Coleman-Derr et al. 2016, Glynou et al. 2016 2018*a*, Thiergart et al. 2020), showing that climatic variables and spatial distance, but not host identity, are major determinants of fungal distribution in plant roots, in a fashion similar to that found in soil (Talbot et al. 2014, Tedersoo et al. 2014). However, large-scale studies have mainly focused on one or few phylogenetically related plant species growing across similar habitat conditions over the sampling ranges, due to the need to standardize surveys over broad distances, or to the restricted niche breadths of the focal plants. Therefore, they provide little insight as to how landscape heterogeneity drives the diversity and function of root-associated fungi. If deterministic processes such as adaptation to specific factors are important for the local assembly of fungal communities (Peay et al. 2016), sampling designs enabling comparisons over highly divergent conditions or plant hosts, while

Manuscript received 11 February 2021; revised 10 May 2021; accepted 7 July 2021; final version received 8 October 2021. Corresponding Editor: Jason D. Hoeksema.
[4] E-mail: jose.maciavicente@wur.nl

properly accounting for co-varying factors, may enhance the chances of identifying ecological preferences in fungi. This, in turn, may help infer the functional implication of root-associated fungi in local or host-specific processes.

Here, we determined how communities of root-associated fungi are affected by environmental conditions, spatial distance, and host identity in different habitat types across a latitudinal gradient in Western Europe. We focused our study on natural and seminatural heathlands and grasslands, which share factors that determine limited nutrient availability and tree cover (Fielding and Haworth 2002, Price 2003) while imposing different constraints to fungal growth. Heathlands have acidic soils abundant in recalcitrant organic matter and with low mineralization rates, where dominant ericaceous shrubs establish ericoid mycorrhizas (ErM) mainly to scavenge organic nitrogen (Read et al. 2004). Grasslands show a broader range of ecological characteristics and types of nutrient limitation (Price 2003, Fay et al. 2015), with dominant grasses and forbs often establishing arbuscular mycorrhizas (AM) to forage for soil phosphorus (Fitter 2005). In turn, fungi–root associations have characteristic patterns of soil colonization. For example, ErM hyphae extend only a few millimeters from host roots while AM can reach several meters as hyphal networks that connect nearby plants, each reflecting a specific strategy to capture resources and associate with hosts (Smith and Read 1997, Tedersoo et al. 2020*b*). Nonetheless, ErM and AM fungal species represent just a small fraction within the root-colonizing fungal communities of heathlands and grasslands (Leopold 2016, Lekberg et al. 2018), among a broad diversity of fungi yet uncharted, both phylogenetically and functionally.

We aimed at testing for habitat and host plant preferences in root-associated fungi, both at the community level and across fungal phylogeny, which may reveal adaptations to and, thereby, implication in specific, local processes. Such adaptations would be evidenced by stable associations of fungal communities with habitats and/or plant taxa across large geographic distances, as well as by phylogenetically clustered assemblages formed by closely related fungi, likely to share functional traits (Webb et al. 2002). We surveyed for root-associated fungi on two scales: continentally, to search for robust associations across varying environments; and locally, to identify small-scale patterns in fungal distribution characteristic for each habitat.

Methods

Field collections

Sampling was performed between April and August 2018 at five geographical locations along a latitudinal gradient in Western Europe, within the Natural Park Los Alcornocales (AL) and the Cabañeros National Park (CB) in Spain, the Black Forest National Park (Schwarzwald; SW) in Germany, the Veluwe region (VE) in The Netherlands, and the Fulufjället National Park (FU) in Sweden (Fig. 1a). In all cases, we obtained sampling permits from local authorities. At each location, we selected two sampling sites, one in one heathland and the other in one grassland (from this point forwards identified by suffixes "_H" and "_G"), separated from each other 1.1, 1.9, 0.04, 0.3, and 0.74 km in AL, CB, SW, VE, and FU, respectively. Both these habitat types were broadly construed as being dominated by Ericaceae shrubs, or by grasses or sedges in the Poales, respectively. At every site, we collected individuals of two plant species within a plot of 16 m^2, divided into 1 m^2 subplots (4×4) delimited by a gridded net (Fig. 1b). We collected one specimen per species and subplot, when possible, by uprooting the entire plant or by digging a root sample, which was individually stored in sterile 50 mL polypropylene tubes together with some root-associated soil. This resulted in a maximum of 16 replicates per plant species and site (i.e., 32 specimens per site), although in several cases fewer replicates were obtained due to absence of a species in some subplots. During collection, we measured the relative x and y distances of specimens respect to the gridded net using a metric tape. We strove to sample in all the heathlands the dominant Ericaceae and Poales species, and in grasslands the dominant Poales and one of the dominant eudicots, to ensure that we retained phylogenetically distant species representing one eudicot and one monocot at every site (Fig. 1c). This was only not possible for SW_G due to the scarcity of forbs and shrubs, and in FU_H where no grasses grew. We identified the plants morphologically and by sequencing their internal transcribed spacer (ITS) rDNA regions using universal or plant-specific primers (White et al. 1990, Cheng et al. 2016). Images of all sampling sites and species are shown in Appendix S1: Fig. S1.

In addition to the plant samples, at each site we collected one subsample of bulk soil per subplot, each consisting of a core of approx. 5 cm diam. and 10 cm depth, and pooled them in one zip-lock bag. Fractions of these soil samples were sent to the Soil Science Laboratory Unit of Goethe University (Frankfurt am Main), where soil chemistry variables were measured using standard protocols. Climatic data for every site were retrieved from the WorldClim database (www.worldclim.org) using package RASTER v2.8-19 of R v3.6.3 (Hijmans 2017, R Core Team 2020). The details of the sampling sites and the plant species collected are provided online at https://doi.org/10.6084/m9.figshare.12988187.

DNA extraction from roots and soil

We started to process the root and soil samples the day after they were collected; only those from CB were processed after two days. Roots were gently shaken to remove loosely adhered soil particles, and then root

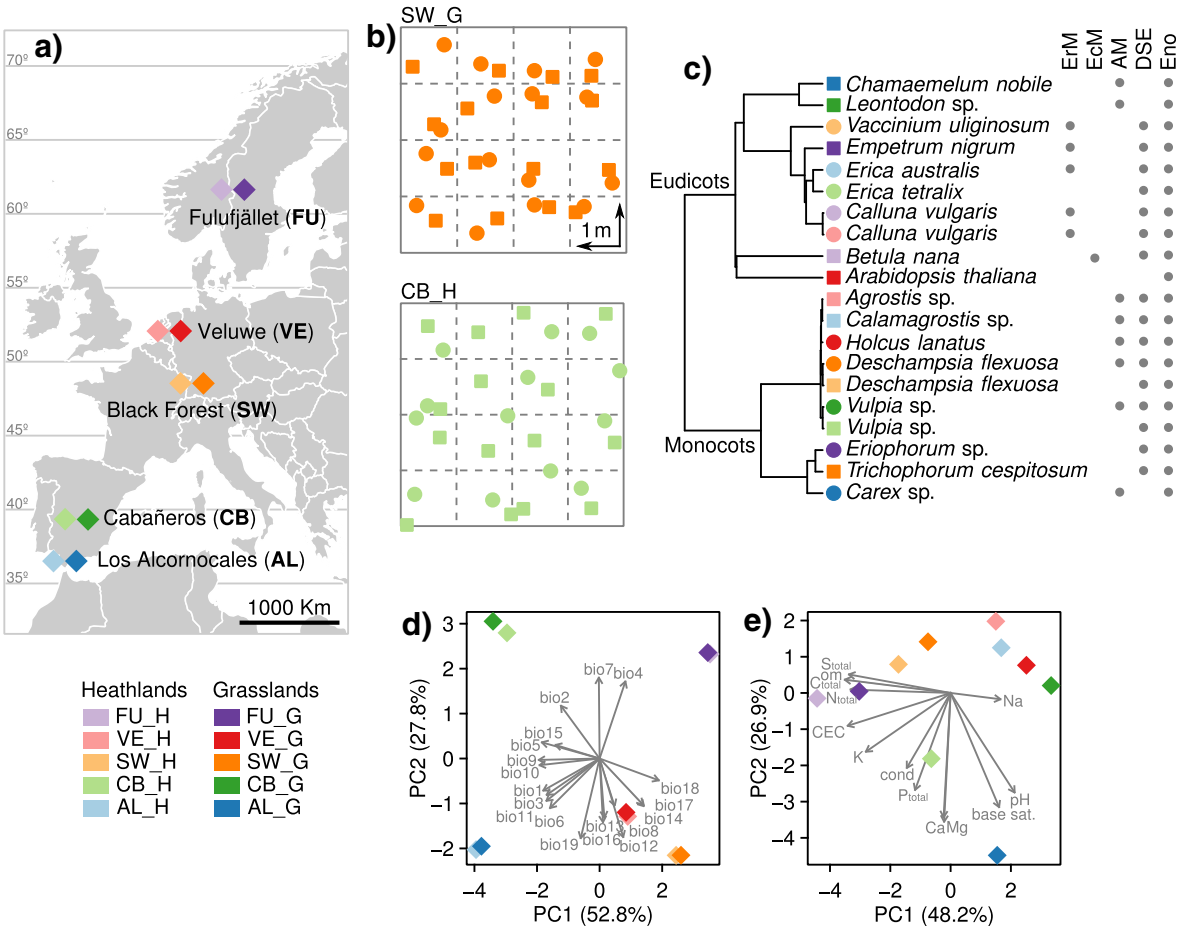

FIG. 1. Sampling design and ecological factors considered in this study. (a) Map showing the sampling sites in five locations following a latitudinal gradient in Western Europe, spanning from southern Spain to central Sweden. At each location, two sampling sites were established within a distance of 2 km, representing one heathland and one grassland. (b) Two examples of the local sampling design at each site. At every site, specimens of two plant species (indicated by different symbols) were collected in a 4 × 4 m square plot, with one individual per species collected within each square meter. The layouts of all sampling sites are provided in Appendix S1: Fig. S6. (c) Phylogenetic tree showing all plant species sampled, with colors indicating the sampling site where they were collected. The two species within each sampling site are indicated with different symbols. Next to each plant are summaries of the main types of root fungal colonization as observed by light microscopy: ericoid mycorrhizas (ErM), ectomycorrhizas (EcM), arbuscular mycorrhizas (AM), dark septate endophytes (DSE), and other endophytes (Endo). (d) Principal component analysis (PCA) ordination of sampling sites according to their bioclimatic conditions, with the position of points indicating relationships among sites, and arrows showing the contribution of each climatic variable to the separation between sites. The position of points is shifted slightly to avoid overlap between points from the same location. (e) PCA ordination of sampling sites according to their soil chemical characteristics, with arrows showing the contribution of each soil variable to the separation between sites. All climatic and soil variables, with explanation of the abbreviations used in the graphs, are provided online at https://doi.org/10.6084/m9.figshare.12988187.

subsamples were cut into pieces approx. 1 cm long and introduced in 2 mL tubes. The root pieces were washed twice in 1 mL sterile phosphate-buffered saline solution (130 mmol/L NaCl, 7 mmol/L Na_2HPO_4, 3 mmol/L NaH_2PO_4, 0.02% Tween 20, pH 7.0) by shaking at 15 Hz for 5 min in a Retsch MM200 mixer mill (Retsch GmbH, Haan, Germany) without beads. The washed roots were transferred to new 2 mL tubes containing 600 µL DNA extraction buffer (2% (w/v) cetyltrimethyl ammonium bromide, 100 mmol/L Tris-HCl, 20 mmol/L EDTA, 1.4 mol/L NaCl, 1% (w/v) 40,000 polyvinyl pyrrolidone, 20 µg/mL RNase A, pH 8.0) and two 4 mm-diameter metal beads, ground in a mixer mill at 25 Hz for 5 min, and frozen at −20°C until use. The soil particles in the supernatant of the root washouts were pelleted by centrifugation at 17,000 ***g*** for 10 min to obtain rhizosphere soil samples, which were then pooled by plant species and site. Rhizosphere soil samples and subsamples of approx. 100 mg from the bulk soils collected at every site were resuspended in 600 µL DNA extraction buffer and processed as explained for the root samples.

Root and soil samples were thawed and incubated at 65°C for 30–45 min, then one volume of 24:1 chloroform:isoamyl alcohol was added and tubes were centrifuged at 17,000 ***g*** for 10 min. The DNA in the supernatant was precipitated in isopropanol at −20°C for 20–40 min, pelleted by centrifugation at 11,000 ***g*** at 4°C for 20 min, washed in ice-cold 70% ethanol, and resuspended in 50 μL nuclease-free water. We measured the quantity and quality of DNA using a NanoDrop spectrophotometer (NanoDrop products, Wilmington, DE, USA) and prepared aliquots of all samples at DNA concentrations of 2 ng/μL. Negative extraction controls were included in every extraction batch and processed with samples in downstream steps.

Fungal amplicon sequencing

We amplified the fungal rDNA ITS region using primers ITS1F and ITS2 (White et al. 1990), modified following Smith and Peay (2014) to include Illumina Nextera adapters, a linker sequence, and 12-bp error-correcting Golay barcodes for multiplexing. PCR reactions were done in 20 μL containing 4 ng of DNA template, 1.5 mmol/L $MgCl_2$, 0.8 mg/mL bovine serum albumin (New England Biolabs GmbH), 0.2 mmol/L of each dNTP (Bioline, Luckenwalde, Germany), 0.2 μmol/L of each primer, and 0.5 units of Phusion Hot Start Flex DNA polymerase (New England Biolabs GmbH). Amplifications were carried out in a Mastercycler pro thermal cycler (Eppendorf, Hamburg, Germany) at 94°C for 1 min followed by 30 cycles of 94°C for 30 s, 52°C for 30 s, and 68°C for 30 s, and a final step of 68°C for 10 min. Negative PCR controls containing water instead of DNA were included in every amplification batch and processed with samples in downstream steps. In addition, two positive controls included equimolar amounts of DNA from 25 fungal isolates obtained from soils collected at the sampling sites, isolated during another study (J. G. Maciá-Vicente, B. Bai, R. Qi et al., *unpublished*).

The uniquely tagged amplicons were quantified in electrophoresis agarose gels and mixed at equimolar amounts in two pools, together with samples from another study. The pooling was done so that all samples from each location were kept together: AL, CB, and SW in one tube, and VE and FU in the other. This way, within-site comparisons were not affected by analytical differences between runs. Distance-based redundancy analysis (db-RDA; Legendre and Legendre 2012) of the samples from the other study, in which treatment replicates were distributed between the two runs, showed that the sequencing run explained a maximum of 1.9% of community variance, and only 0.15% when the treatment effects were accounted for. In total, this study included amplicons from 294 root samples, 20 rhizospheric soils (one per host plant), 10 bulk soils (one per sampling site), five of each DNA extraction and PCR negative controls, and two positive controls. The DNA pools were purified using the Zymoclean^{TM} Gel DNA Recovery Kit (Zymo Research, Freiburg, Germany), quantified with a Qubit Fluorometer (Thermo Fisher Scientific, Waltham, Massachusetts, USA), and paired-end sequenced by Eurofins Genomics GmbH (Ebersberg, Germany) on the Illumina MiSeq platform, using the MiSeq Reagent Kit v3 (Illumina Inc., San Diego, California, USA).

Processing of ITS reads

We processed the assembled sequence reads using the DADA2 pipeline for quality filtering, dereplication, removal of chimeric sequences, grouping into amplicon sequence variants (ASVs; Callahan et al. 2017), and producing an ASV-per-sample contingency table (Callahan et al. 2016, 2017). This pipeline has proven sensitive and accurate for analyzing fungal community datasets generated by MiSeq amplicon sequencing (Pauvert et al. 2019). However, to assess possible effects of the bioinformatics processing in the results, most analyses were repeated using other popular pipelines based on USEARCH (Edgar 2010) and UNOISE3 (Edgar 2018). These yielded similar downstream results to those obtained by our choice pipeline (Appendix S1: Fig. S2). We used BLASTN v2.2.31+ to compare ASVs against all NCBI GenBank records as of August 2019 and remove non-fungal sequences. Fungal ASVs were then taxonomically annotated by comparing against the UNITE database of fungal ITS sequences (Kõljalg et al. 2005) using the Naïve Bayesian Classifier tool (Wang et al. 2007) available in MOTHUR v1.39.5 (Schloss et al. 2009). Negative controls contained only seven ASVs, five in the extraction and two in the PCR controls, of which only two had more than 10 total reads (Appendix S1: Fig. S3). All ASVs found in the negative controls were removed from the dataset. Prior to further analyses, ASVs were grouped into operational taxonomic units (OTUs) at a 99% similarity threshold using CD-HIT v4.6 (Fu et al. 2012), with consensus taxonomy assignments per OTU obtained from the ASV annotation with the *classify.otu* tool of MOTHUR. We used the taxonomic assignments to generate a hierarchical classification tree of OTUs for phylogenetic ecological analyses, by subsetting the backbone classification tree provided by Tedersoo and co-workers (Tedersoo et al. 2018) for fungi, using the R package PHYLOCOMR v0.1.2 (Ooms and Chamberlain 2018). We identified OTUs putatively belonging to ErM, ectomycorrhizal (EcM), or AM fungi using FUNGuild v1.0 (Nguyen et al. 2016), by selecting taxa with a likelihood of belonging to each guild as "Probable" or "Highly Problable." We discarded OTUs with less than five overall reads before downstream analyses, and two samples with <100 total reads (VE_H_2_3 and FU_H_1_1). Our selection of a 99% similarity cut-off threshold to define OTUs was aimed to enable separation of closely related species (e.g., see Maciá-Vicente et al. 2020*b*). Nevertheless, data analyses using OTUs

defined at a 97% similarity resolutions, or ASVs, yielded comparable downstream results (Appendix S1: Fig. S2).

Analysis of the mock community in positive controls at different similarity thresholds for OTU clustering showed that, in every case, most isolates were split into several OTUs (Appendix S1: Fig. S3). In addition, 7 of the 25 isolates were not detected using any threshold (Appendix S1: Fig. S3), which could result from sequence inserts in the ITS1 region of these fungi hampering the assembly of read pairs (Cross et al. 2017).

Light microscopy of roots

Root subsamples *c*. 5-cm long from all specimens were pooled per plant species and site in one polypropylene tube and cleared for 24–48 h in 10% (w/v) KOH at room temperature. After that, roots were washed with distilled water, acidified for 20 s in 3% (v/v) HCl, washed again, stained overnight in a 0.4% (w/v) Trypan blue solution (Amresco, Solon, Ohio, USA) in an orbital shaker at 180 rpm, and finally de-stained for 24 h in lactoglycerol under shaking. Root pieces of *c*. 0.5 cm in length were mounted on microscope slides with lactoglycerol, squashed with a cover slip, and observed under a Zeiss Axio Lab.A1 light microscope equipped with an Axiocam Erc 5s camera (Zeiss, Hamburg, Germany). We screened between 5 to 8 root pieces per plant species and recorded different types of fungal–root colonization such as undifferentiated hyphae, mycorrhizal structures, or microsclerotia.

Analyses of community diversity and composition

We assessed sampling completeness in individual samples using rarefaction curves (Appendix S1: Fig. S4) built with functions in the package VEGAN v2.5-4 of R (Oksanen et al. 2019). To normalize total read abundances per sample and account for differences in library size, we relied on a mixture model using the variance stabilization method available in the R package DESEQ v1.35.1 (Anders and Huber 2010). The latter approach has been shown to outperform rarefying-based normalization, in that it does not require dropping samples or OTUs with low abundances, and does not decrease the statistical power in analyses (McMurdie and Holmes 2014). We compared community composition across root and soil samples by obtaining Bray–Curtis dissimilarities and visualizing them with a non-metric multidimensional scaling (NMDS) ordination. Taxonomic summaries at the order and phylum level were obtained per species and site, and ordered using a dendrogram based on Bray–Curtis dissimilarities among samples at the order level. The relative abundances of the main fungal orders across root, rhizosphere, and bulk soil samples, and across sampling sites were compared using the Kruskal–Wallis rank sum test, and the Benjamini–Hochberg method to adjust *P*-values after multiple comparisons. Diversity indexes including observed richness, Shannon diversity, and Simpson's diversity per root sample were calculated using functions in VEGAN. In addition, we used the OTU classification tree to calculate phylogenetic diversity measures using functions in package PICANTE v1.8 (Kembel et al. 2010), including Faith's phylogenetic diversity, the net relatedness index (NRI), and the nearest taxon index (NTI) per sample (Webb 2000). Phylogenetic diversity equals the sum of the branch lengths for all OTUs per sample, whereas NTI and NRI measure different aspects of phylogenetic clustering vs. overdispersion in OTUs within a community. The values measured for phylogenetic diversity indexes were compared with those obtained from null communities, designed by randomizing OTUs per sample to calculate standardized effect sizes (z), as an estimation of whether communities are more phylogenetically clustered or overdispersed than expected by chance (Webb 2000). We compared diversity variables between heathlands and grasslands by including them as fixed effects in linear mixed-effects models built with the R package LME4 v1.1-21 (Bates et al. 2015). These included the factor location as random slopes and intercepts to account for pseudoreplication. In these models, we weighted richness and Shannon index with read abundances as covariates, and phylogenetic diversity with richness, due to the strong correlation between these pairs of variables (Pearson's $r = 0.84$, 0.37, and 0.98, $P < 0.001$, respectively). We calculated partial standardized residuals for each variable and tested for differences between both habitat types using likelihood ratio tests, by comparing with models without the variable in question.

Effect of ecological variables on community structure

We used variance partitioning analysis to assess the effects of climate, soil conditions, geographical distance, habitat type, and host phylogeny on the composition of fungal–root communities across sampling sites. This relied on db-RDAs of Bray–Curtis dissimilarities calculated among pairs of samples representing pooled reads per site and plant species, to avoid pseudoreplication. To include climatic and soil conditions, we carried out principal components analysis (PCA) for each dataset using scaled variables, and included the first two components of each ordination as explanatory variables in the db-RDAs (Fig. 1d,e). We included latitude and longitude coordinates to represent geographical distance, and habitat type (heathlands and grasslands) as a vector of zeros and ones. We included host phylogeny following the approach described by Desdevises et al. (2003). For that, we first obtained a phylogenetic tree containing all host plants by subsetting the tree provided by Zanne et al. (2014), which includes nearly all plant genera. We then calculated a principal coordinates analysis with the cophenetic tree distances, retaining the first two axes as described above for climatic and soil variables. These two axes represent 82.9% of phylogenetic variance across

hosts, most of it (73.8%) compiled in the first axis that mainly separates eudicots from monocots (Appendix S1: Fig. S5). We measured the relative contribution of each set of explanatory variables by sequentially removing explanatory variables from the db-RDA models and recording the resulting changes in the total variance explained (Legendre and Legendre 2012). A temporal component (date of sampling) was not included in these analyses because it was strongly collinear with latitude ($r = 0.87$, $P = 0.001$), plus variance partitioning showed that it only explained a non-significant ($P > 0.05$) 2.8% of community variation after spatial distance, climate, and soil conditions were accounted for.

Measurement of fungal distribution ranges

We measured the distribution ranges for every OTU at both continental and local scales. In the first case, we calculated the maximum distance between the sampling sites where each OTU was found. For the local scale, we calculated the maximum distance between the plant specimens where each OTU was found within every sampling site, using the coordinates respect to the gridded net recorded upon sampling. To disentangle the interaction between local abundances and spatial distribution that is common to natural communities (Brown 1984, Egidi et al. 2019), we assessed possible relationships between continental and local distribution ranges and OTU abundances per plant using linear or quadratic regressions, which were selected in each case based on the Akaike's Information Criterion to retain the best-fitting model. Potential relationships between OTU numbers and distribution ranges for different fungal orders were tested with the Spearman's correlation test.

Evaluation of fungal host preferences

We evaluated the effects of host identity on community composition and on the occurrence of individual OTUs independently for each sampling site. In every case, we first applied variance partitioning analysis as explained above, using spatial factors and host identity as explanatory variables. We assessed the former to account for possible sources of variation in community structure due to spatial heterogeneity within each site, which could interfere with effects purely due to host identity. They were included as principal coordinates of neighbor matrices (PCNM) vectors (Legendre and Legendre 2012), calculated from the local coordinates of each specimen recorded upon sampling, using the function *pcnm* of VEGAN. Only the PCNMs that explained the maximum amount of community variance per site were retained by applying forward and backward variable selections. Host identity was included as a numerical vector of zeros and ones, each representing one of the two plants per site.

To identify the effects of host identity on individual OTUs, we applied multispecies generalized linear models (GLMs) using the function *traitglm* in the R package MVABUND v4.0.1 (Wang et al. 2012). We used this to fit GLMs to individual OTU abundances, while simultaneously accounting for interactions across OTUs (Warton et al. 2015). We also accounted for spatial factors as indicated above, by selecting the two most explanatory PCNMs in each site using MVABUND's function *best.r.sq*, and including them as covariates. Within each site, models only included OTUs that occurred in a minimum of six plant specimens, and relied on negative binomial distributions of non-normalized (count) read abundances, including a row effect to adjust for different sampling intensities across samples. We extracted from models the interaction coefficients relative to host plants, indicating whether occurrence of each OTU was positively or negatively associated with any of the two hosts. The models were configured to apply LASSO penalties to coefficients, which set to zero interaction coefficients not contributing significantly to results upon model selection (Warton et al. 2015). In every site, negative values indicated significant associations with the monocot host, and positive values with the eudicot host. The only exception was for sites SW_G and FU_H, where two monocots and two eudicots were collected, respectively. We tested for phylogenetic signal in the host coefficients across fungal phylogeny using Blomberg's K (Blomberg et al. 2003), measured with function *phylosig* in R package PHYTOOLS v0.6-99 (Revell 2012).

Lastly, we attempted to quantify the relative importance of different ecological processes in the assembly of the fungal communities in each site using the R package ICAMP v1.3.4 (Ning et al. 2020). The method partitions the variance in community phylogenetic diversity into deterministic processes (i.e., selection by the host plant), based on its relationship with biotic and abiotic variables; and into stochastic processes (i.e., dispersal and drift) by further dividing the variance not explained in the previous step (Zhou and Ning 2017).

Data and code availability

The Illumina MiSeq sequence data generated in this study were deposited in the NCBI Sequence Read Archive under BioProject number PRJNA640064. The ITS sequences used for the identification of host plants were deposited in NCBI GenBank under accessions MT376778–MT376821. All the data and code used for the analyses are available online at https://doi.org/10.6084/m9.figshare.12988187.

Results

Survey of root-associated fungi at continental and local scales

We collected roots from plants in heathlands and grasslands at five locations distributed along a latitudinal gradient in Western Europe (Fig. 1a). Because each

site hosted a unique plant community, we selected different plant species per site among the two most frequent locally, to a total of 17 species for the 10 sampling sites (Fig. 1c). Classification of the sites using PCA of some bioclimatic variables showed a strong pairing by geographic location, due to the closely similar conditions at adjacent sites (Fig. 1d). Maximal differences are displayed by the PC1 axis between both locations in Spain and the rest, mainly driven by warmer temperatures (e.g., bio1, bio5, bio9, bio10) in the former, and then by PC2 that separates CB and FU from the other locations based on their wider temperatures ranges (e.g., bio4, bio7) and lower precipitation (e.g., bio12, bio13, bio16, bio19; Fig. 1d). Differences among sites based on chemical properties of bulk soil also showed a degree of pairing between sites by location, except for AL and CB (Fig. 1e). Separation was strongest following variables associated with the content of soil organic matter, such as contents of nitrogen, carbon, and sulfur, all reaching maximum values in both sites at FU and followed by those at SW. Indeed, the amounts of organic matter in both FU soils were more than double those in other sites (82.1 and 75.5% of total soil weight, vs. 37.4 and 33.4% in SW), to the extent that the low quantity of inorganic soil constituents in the FU_G sample precluded the measurement of several soil parameters (see data online at https://doi.org/10.6084/m9.figshare.12988187). The second axis of variation separated CB_G and AL_H from the rest, based on variables associated with higher pH, such as high quantities of the base cations calcium and magnesium (Fig. 1e).

The sampling design enabled uncoupling of location-related variables at the continental scale, with climatic and soil variables yielding distinct similarity patterns that do not fully reflect geographic distances (Fig. 1a,d,e). The selection of phylogenetically distant pairs of plant species by site enables the detachment of the factor host plant from other ecological factors, even when different species are collected across areas (Fig. 1c). Sampling schemes within sites were set so that no interference existed between the factor host plant and local sources of variation acting on fungal communities, such as clustering patterns of plant specimens across the area; or that heterogeneity in local conditions can be accounted for (Appendix S1: Fig. S6).

The type of associations between fungi and roots vary across host phylogeny and habitats

Direct observation of fungal structures in roots showed several main types of conspicuous associations that were differently distributed across host species and sampling sites (Fig. 1c). Roots were often surrounded by mantles or dense nets of hyphae (Fig. 2a–d), especially in heathland eudicots but less apparent in grasslands, and nearly absent in forbs. We classified the types of root association according to diagnostic characters (Smith and Read 1997), as ErM formed by densely packed hyphal complexes within epidermal cells of ericoid roots (Fig. 2e–i); EcM, with root tips tightly enclosed by hyphal mantles; AM, identified by the presence of intraradical vesicles (Fig. 2j,k), arbuscles, or abundant, thick, and unseptated running hyphae; dark septate endophytes (DSE), characterized by melanized hyphae and microsclerotia (Fig. 2l–s); and other endophytes, mainly represented by undifferentiated, hyaline hyphae (Fig. 2t–x). Unsurprisingly, ErM were only found in ericaceous roots, including *Empetrum nigrum* L. collected at the FU grassland (Fig. 2i), but we did not find them in *Erica tetralix* L. from CB_H. *Erica australis* L. from AL_H showed ErM structures morphologically different to those observed in other heathlands, with hyaline hyphae forming a mantle surrounding roots (similar to that described by Vohník et al. 2012) that contrasted with tangled dematiaceous hyphae in other cases (compare Fig. 2a and 2b); and less packed intracellular hyphal complexes (compare Fig. 2e with 2f–i). Only *Betula nana* L., collected in FU_H, showed EcM (Fig. 1c). We observed AM in all grassland grasses and forbs, with the exception of *Arabidopsis thaliana* (L) Heynh., and also in grasses collected at the AL and VE heathlands (Fig. 1c). DSEs were spotted in nearly all cases, with the exception of the grassland forbs and *Carex* sp. at AL_G, whereas we detected hyaline endophytes in all roots observed (Fig. 1c). The latter endophytes were the exclusive association type found in *A. thaliana*.

Continental-scale drivers of root-associated fungal communities

We profiled the fungal communities associated with roots of all plant specimens sampled (n = 294), their rhizospheres (pooled by plant species and site; n = 20), and bulk soils from each site (pooled by site; n = 10) using Illumina MiSeq sequencing of ITS amplicons. We obtained a total of 11,422,480 quality-filtered reads from two sequencing runs, with a median of 29,151 and a standard deviation of 26,783 reads per root sample, and of 9,778 and 13,916 per soil sample. Reads were grouped into 10,010 ASVs that we further grouped into 7,703 OTUs based on 99% sequence similarity, of which 6,566 and 2,373 OTUs were detected in root and soil samples, respectively. Similar downstream results were obtained when using clustering thresholds ranging from 97% similarity to the ASV level (Appendix S1: Fig. S2).

Comparisons of community structure using a NMDS ordination (stress = 0.14) of Bray–Curtis dissimilarities showed that fungal assemblages were strongly site specific (Fig. 3a), with samples forming compact clusters by site irrespective of whether they originate from roots, rhizosphere, or bulk soil. No clear separation between heathlands and grasslands was evident, notably due to the close similarity between both habitat types at SW and FU, and despite the fact that grassland samples from all other locations clustered to the right in the

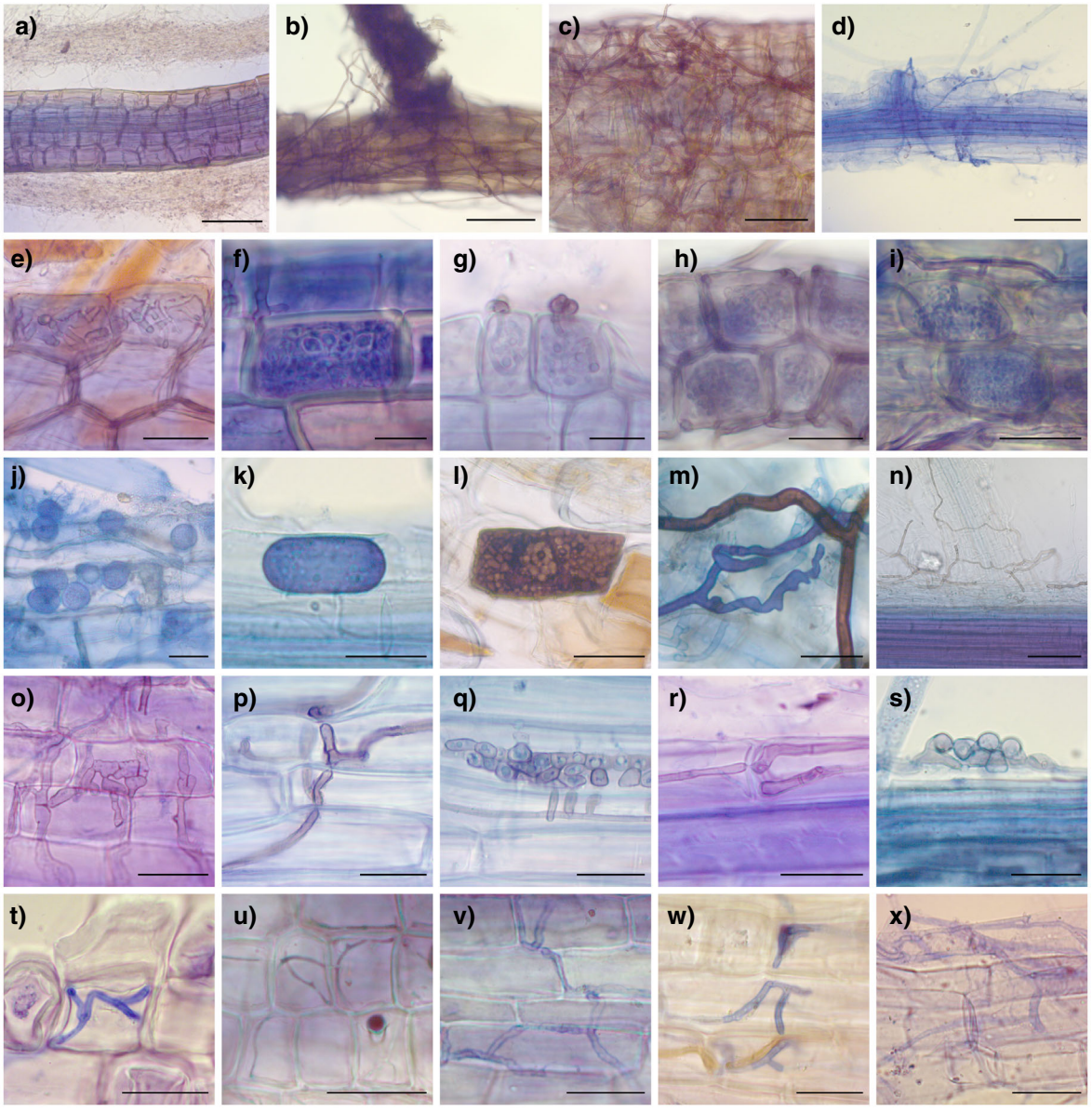

FIG. 2. Microscope characteristics of fungi–root colonization across host plants and sites. (a–d) Overview of root surface colonization in different hosts and sites: *Erica australis* in AL_H (a), *Empetrum nigrum* in FU_G (b), *Betula nana* in FU_H (c), and *Agrostis* sp. in VE_H (d). (e–i) Intracellular hyphal coils in specialized epidermal root cells indicative of ericoid mycorrhizal associations: *E. australis* in AL_H (e), *Vaccinium uliginosum* in SW_H (f), *Calluna vulgaris* in VE_H (g) and FU_H (h), *E. nigrum* in FU_G (i). (j, k) Intraradical vesicles of arbuscular mycorrhizal fungi in *Calamagrostis* sp. in AL_G (j) and *Holcus lanatus* in VE_G (k). (l–s) Dark septate endophyte (DSE) morphologies in root-colonizing fungi: intracellular microsclerotium in *Erica tetralix* in CB_H (l), epiphytic hyphae in *C. vulgaris* in VE_H (m) and *Vulpia* sp. in CB_H (n), endophytic hyphae in *Deschampsia flexuosa* in SW_H (o), intracellular hypha (p) and microsclerotium (q) in *Eriophorum* sp. in FU_G, endophytic hypha in *Agrostis* sp. in VE_H (r), epiphytic microsclerotium in *H. lanatus* in VE_G (s). (t–x) Endophytic root colonization by hyaline fungi: *Trichophorum cespitosum* (t) and *D. flexuosa* (u) in SW_G, *D. flexuosa* in SW_H (v), *Eriophorum* sp. in FU_G (w), *Arabidopsis thaliana* in VE_G (x). Bars: a, b, d, n = 20 μm; c, e, l = 10 μm; h–k, m, o–x = 5 μm; f, g = 2.5 μm.

graph (Fig. 3a). Samples were neither separated within each site between host plants, with the only exception of CB_H for which samples from the two species formed distinct clusters (Fig. 3a). A similar pattern to that shown by samples was reproduced by the OTU scores (Fig. 3b), which formed clusters for every site that suggested that most OTUs are site specific, while very few OTUs are shared between samples placed leftwards and rightwards in the graph. However, the majority of the 85 most abundant genera (with a minimum of 0.1% of the

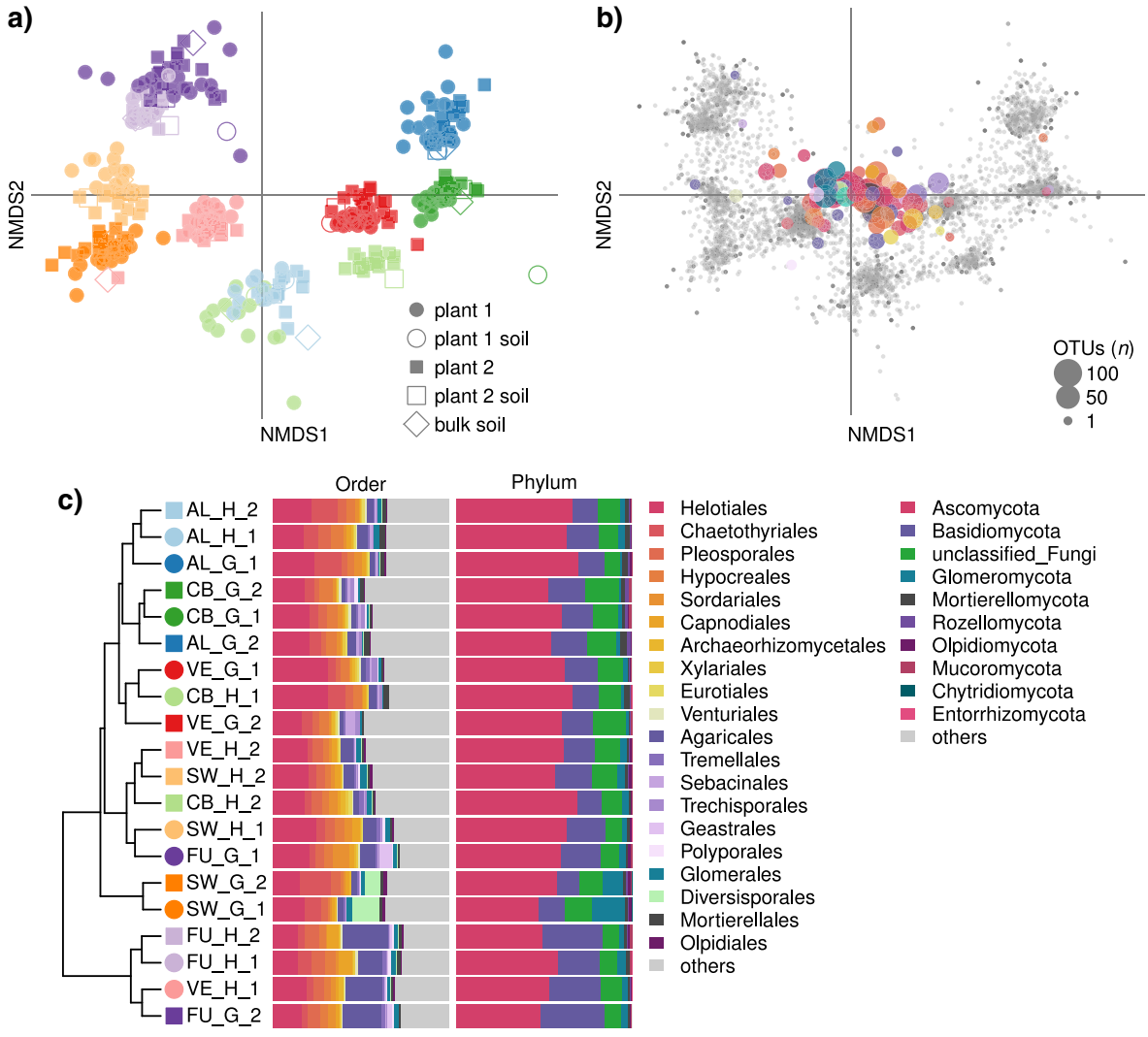

FIG. 3. Structure and composition of fungal communities in roots. (a) Non-metric multidimensional scaling (NMDS) based on Bray–Curtis dissimilarities showing relationships in fungal community structure among individual root and soil samples collected in 10 sites and five locations. Points correspond to individual samples, with shape differentiating the two plant collected at each site or the type of soil sample, and color indicating the sampling site. For a color key of plants and sampling sites, see the dendrogram in (c). (b) OTU scores for the NMDS plot in (a) showing the relationships between OTUs in fungal communities. Gray points correspond to individual OTUs. Colored points represent the centroids for all OTUs of each genus represented by a minimum of 0.1% of the total reads. Point colors indicate the fungal order to which the genera belong to (see color key in c), whereas point sizes are relative to the total number of OTUs in each genus. (c) Distribution of fungal orders and phyla across host plants and sampling sites. The samples are ordered according to a dendrogram based on Bray–Curtis dissimilarities calculated on order abundances across samples. Only the 20 identified orders with the highest overall abundance, and the 10 phylum-level ranks, including unidentified fungi, are represented in bar plots.

total reads) are widespread, with 29 genera (34.1%) occurring at all sites, 75 (76%) at a minimum of five sites, and only one (1.1%) genus occurring at a single site (see data online at https://doi.org/10.6084/m9.figshare.12988187). This is shown in the NMDS plot by the clustering in the middle of the graph of most centroids for all OTUs within each genus (Fig. 3b); the few genera that appear to be specific from one or two sites are solely represented by one OTU. The patterns in the NMDS ordination are robust even when the analysis is repeated after removing all OTUs found exclusively in one site, and therefore are not driven by endemic fungi (Appendix S1: Fig. S7).

We used variance partitioning of db-RDAs to measure the relative contribution of ecological variables to community structure. In these, we used as explanatory variables the two main axes of PCAs in Fig. 1d,e to represent climate and soil conditions, respectively;

geographic coordinates to represent spatial distance; habitat type; and two principal coordinates extracted from the tree in Fig. 1c to summarize host phylogeny (82.9% variance explained, Appendix S1: Fig. S5). Results confirmed the observations in the NMDS concerning the low contribution of habitat type and host plant to community assembly, both in roots and rhizosphere, which mainly depended on local climatic and soil conditions and, to a lesser extent, on spatial distance among sites (Table 1). The relatively small differences between the overall variance explained by every factor and that exclusively explained once the contribution of other factors was accounted for, illustrates the lack of interaction among factors achieved by our sampling design.

Fungal communities were clearly dominated by Ascomycota fungi, which amounted to 57%, 56%, and 60% of total read abundances in roots, rhizosphere, and bulk soil, respectively, and were distantly followed in representation by the Basidiomycota, with 25%, 29%, and 21% of total abundances. At the taxonomic order rank, overall abundances were greatest for fungi in the Helotiales and Agaricales, followed by the Chaetothyriales, Hypocreales, and Pleosporales, all showing similar abundances across roots, rhizosphere, and bulk soil ($X^2(2) = 0.1–8.2$, $P_{adj} > 0.05$; Appendix S1: Fig. S8). In addition, every order with an overall relative abundance above 0.1% (30 out of 131 order-level taxa) was represented at all sampling sites. The dominance patterns at the order and phylum levels followed similar trends in all root samples (Fig. 3c), although no fungal order varied significantly in relative abundance across habitat types or host plants ($X^2(9) = 3.2–24.7$, $P_{adj} > 0.05$). There were, however, specific groups markedly varying in particular samples (Fig. 3c), such as the Agaricales, with overall higher abundances in all shrubs sampled at VE and FU ($X^2(1) = 10$, $P = 0.002$); or AM fungi in the Diversisporales, enriched in both grasses collected at SW_G ($X^2(1) = 6$, $P = 0.01$). Classification of root samples using Bray–Curtis dissimilarities at the order level showed a mixed clustering pattern resulting from the interaction between habitat types and location, similar to that observed using OTU-based dissimilarities (Fig. 3c). Similar patterns in the distribution of orders and phyla across sites and plants were observed in the rhizosphere and bulk soil samples (Appendix S1: Fig. S8).

Heathland and grassland fungal–root communities are phylogenetically clustered

Fungal richness differed between habitat types, with heathlands showing greater OTU numbers per sample than grasslands after accounting for the variation across geographic locations, as well as for differences in read abundances per sample (Fig. 4a). When looking at different locations separately, this pattern was followed by all cases except for sites at CB (Appendix S1: Fig. S9). Similarly, the same pattern was observed when comparing diversity as measured by Shannon ($X^2(1) = 4.01$, $P = 0.045$) and Simpson's ($X^2(1) = 2.82$, $P = 0.093$) indexes (Appendix S1: Fig. S9). However, phylogenetic diversity followed the opposite trend (Fig. 4b), indicating an overall greater phylogenetic similarity among OTUs in heathlands (i.e., higher phylogenetic clustering) than in grasslands. In both cases, the standardized effect sizes (z) of phylogenetic diversity relative to that in a null community with a random distribution of OTUs tended to be negative (median z values of -0.8 and -0.15 for heathlands and grasslands, respectively; Appendix S1: Fig. S9), indicating that communities are more phylogenetically clustered than expected by chance. Similarly, NRI (Fig. 4c) and NTI (Fig. 4d), which measure alternative aspects of community phylogenetic clustering vs. overdispersion, yielded positive values when compared with null communities (median z for NRI of 0.66 and 0.21, and of NTI of 0.79 and 0.23 for heathlands and grasslands, respectively; Appendix S1: Fig. S9), indicating stronger clustering than expected by chance. Both NRI and NTI were greater for heathlands than for grasslands after accounting for differences across locations (Fig. 4c,d), indicating a higher degree of clustering

TABLE 1. Variation of the broad-scale structure of root-associated fungal communities explained by ecological factors.

	Roots				Rhizosphere			
	Combined†		Exclusive‡		Combined		Exclusive	
	Adjusted R^2	P	Adjusted R^2	P	Adjusted R^2	P	Adjusted R^2	P
All	0.63	0.001	n.d.	n.d.	0.50	0.001	n.d.	n.d.
Climate	0.22	0.001	0.23	0.001	0.18	0.001	0.19	0.004
Soil	0.21	0.001	0.22	0.002	0.18	0.001	0.19	0.003
Distance	0.18	0.001	0.15	0.007	0.15	0.001	0.15	0.015
Habitat	0.05	0.014	0.06	0.055	0.03	0.05	0.05	0.123
Host	0.02	0.28	0.01	0.378	0.00	0.458	0.00	0.491

Note: n.d., not determined.
† Overall variance explained by each set of factors.
‡ Variance explained by each set of factors after accounting for the variance explained by other factors.

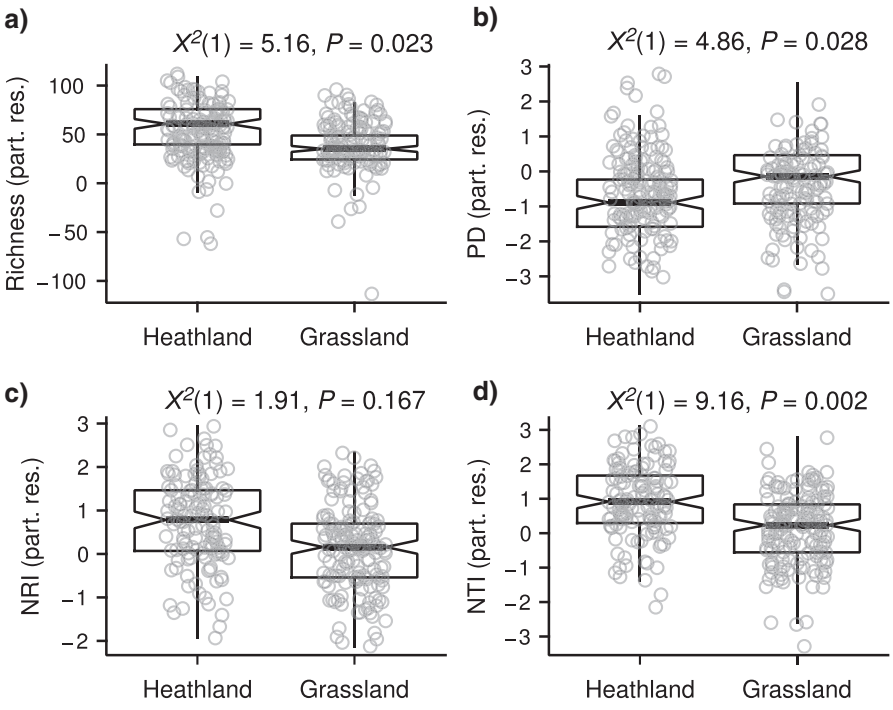

FIG. 4. Comparison of different measures of fungal diversity between heathlands and grasslands. (a) Richness. (b) Faith's phylogenetic diversity (PD). (c) Net relatedness index (NRI). (d) Nearest taxon index (NTI). Plots show partial residuals for each measure, after accounting in linear mixed-effects models (LMEM) for random effects between different samples at each location, and for read abundances and OTU richness in the cases of richness and PD, respectively. Boxplots summarize the distribution of each measure, and points represent individual samples. Statistical differences between habitat types were calculated by means of likelihood ratio tests applied to LMEM.

in heathlands. Nevertheless, only NTI was significant, which suggests that the phylogenetic clustering is more pronounced in terminal branches across the phylogeny, i.e., it is mainly explained by co-occurring sister OTUs. When compared at every site, the patterns in phylogenetic diversity and NTI were consistent across locations (Appendix S1: Fig. S9).

Endemism characterizes the distribution of root-associated fungi

We assessed the individual distribution ranges of root-associated fungal OTUs at two scales: continentally, to study the potential geographic constraints to their occurrence (e.g., due to dispersal or environmental filters); and locally within each sampling site, to infer their patterns of biomass allocation as a potential proxy for their strategies of interaction with plants. At the broadest scale, 4,888 (74%) OTUs had a range of 0 km, indicating that they are site specific, whereas 5,341 (81%) were found within a 2 km area, indicating that they are location specific (Fig. 5a). Only 79 OTUs (1.2%) had distribution ranges above 3,000 km and therefore spanned the area covered by our survey (see data online at https://doi.org/10.6084/m9.figshare.12988187). A similar distribution of OTU ranges was obtained when using more stringent parameters to filter MiSeq reads, therefore discounting that the pattern arises from methodological artifacts (Appendix S1: Fig. S10). Moreover, the relationship between OTU distribution ranges and read abundances by sample are best explained by a negative quadratic model, although little association was found between both variables (adjusted $R^2 = 0.02$, $P < 0.001$; Fig. 5a), therefore suggesting that the pattern was due to true endemicity rather than to rarity of OTUs; i.e., OTUs with very restricted distributions do not have low local abundances compared with widespread OTUs. The continental-scale pattern of OTU distribution was partly reproduced at the local scale in all sampling sites, where 41–51% of OTUs had ranges of occurrence of 0 m and therefore occur in a single plant specimen, while the remaining OTUs were spread throughout all other distance range classes (Fig. 5b). Locally, there were stronger associations between OTU distributions and abundances than continentally (Fig. 5b), although these were still feeble based on positive quadratic relationships (adjusted $R^2 = 0.05$–0.14, $P = 0.001$), or on a positive linear relationship for FU_H (adjusted $R^2 = 0.09$, $P < 0.001$).

To identify taxa with potentially distinct abilities to disperse across small and large distances, we compared the number of OTUs by fungal order at arbitrarily chosen distance classes, representing partitions within sampling sites (0–5 m) and over the entire sampling range

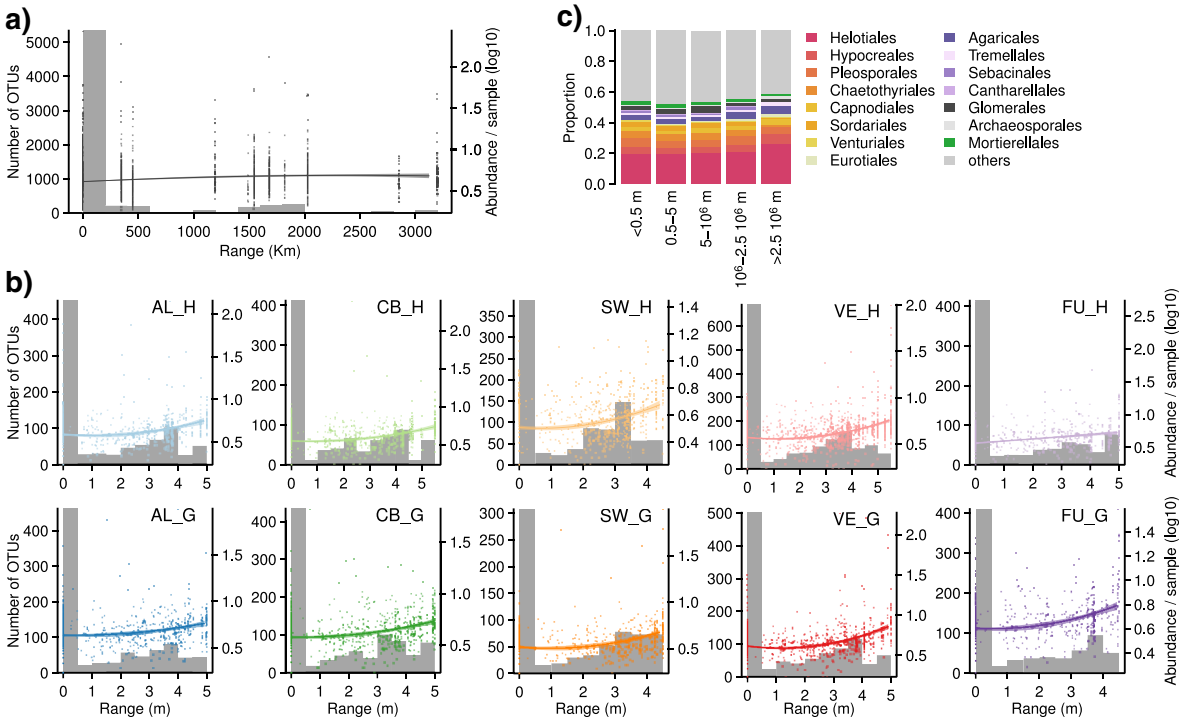

FIG. 5. Distribution ranges of root-associated fungi at continental and local scales. (a) Histogram showing the continental-scale distribution ranges of OTUs. The points superimposed to the histogram represent the individual abundances per plant sample of each OTU, in $\log_{10}$ scale. The line represents a fitted quadratic model of OTU abundances respect to distribution ranges, and the shaded area around it comprises the 95% confidence intervals. (b) Local-scale distribution of OTUs at each sampling site, with histograms, points, and lines showing distribution ranges per OTU and their relationships with OTU abundances. All lines represent quadratic models, except for the one in site FU_H that is based on a linear model, each chosen by selection of the most explanatory model. (c) Relative proportion of OTU numbers for the 15 fungal orders with the highest overall number of OTUs across distance ranges. The distance ranges shown are arbitrary, chosen to represent both local and broad scales.

(from 5 m to >2,500 km). Overall, no major differences in OTU numbers per fungal order could be identified across distance classes (Fig. 5c), as each class somewhat reflects the total proportion of OTUs per taxon for the entire survey. Spearman's rank correlations showed that no fungal order has a significant change with distance in the number of OTUs ($P_{adj} > 0.05$).

Host preferences in root-associated fungi are not phylogenetically conserved

We measured the effect of host identity on the assembly of root-associated fungal communities independently for each sampling site, so that comparisons always involved two phylogenetically distant plant species representing eudicots and monocots, except for SW_G and FU_H where two monocots and two eudicots were collected, respectively. In every site, the specimens of each species were homogeneously distributed across the sampling area (Appendix S1: Fig. S6) to prevent potential effects of spatial clustering in the results. Partition of community variances across spatial (Appendix S1: Fig. S11) and host factors indeed showed a very limited influence of spatial effects on the data, with a maximum adjusted R^2 of 0.05 in FU_G, and values of zero in both sites at CB and SW (Fig. 6a). The variance explained by host alone, after accounting for spatial factors, ranged between 0 in FU_H and 0.33 in CB_H, the latter value representing more than twice the second highest value (adjusted $R^2 = 0.14$ in SW_H, Fig. 6a), which confirmed the clear separation by host observed for CB_H in Fig. 3a. Notably, the sites where host identity explained the least variance in community assembly were SW_G (adjusted $R^2 = 0.03$) and FU_H (adjusted $R^2 = 0$), where phylogenetic distance between host species is minimal. In all other cases, root samples were clearly separated by host plant in db-RDAs (Appendix S1: Fig. S11).

To investigate the differential ability of host plants to recruit fungi, we applied individual GLMs to all OTUs occurring in a minimum of six plant specimens per site, using plant identity as explanatory variable, and accounting for spatial variation within the sampling areas. We retained the standardized model coefficients relative to the host plant, with positive values indicating significant OTU associations with the eudicot, and negative values with the monocot host in every site (Fig. 6b). The exceptions were SW_G and FU_H, where positive

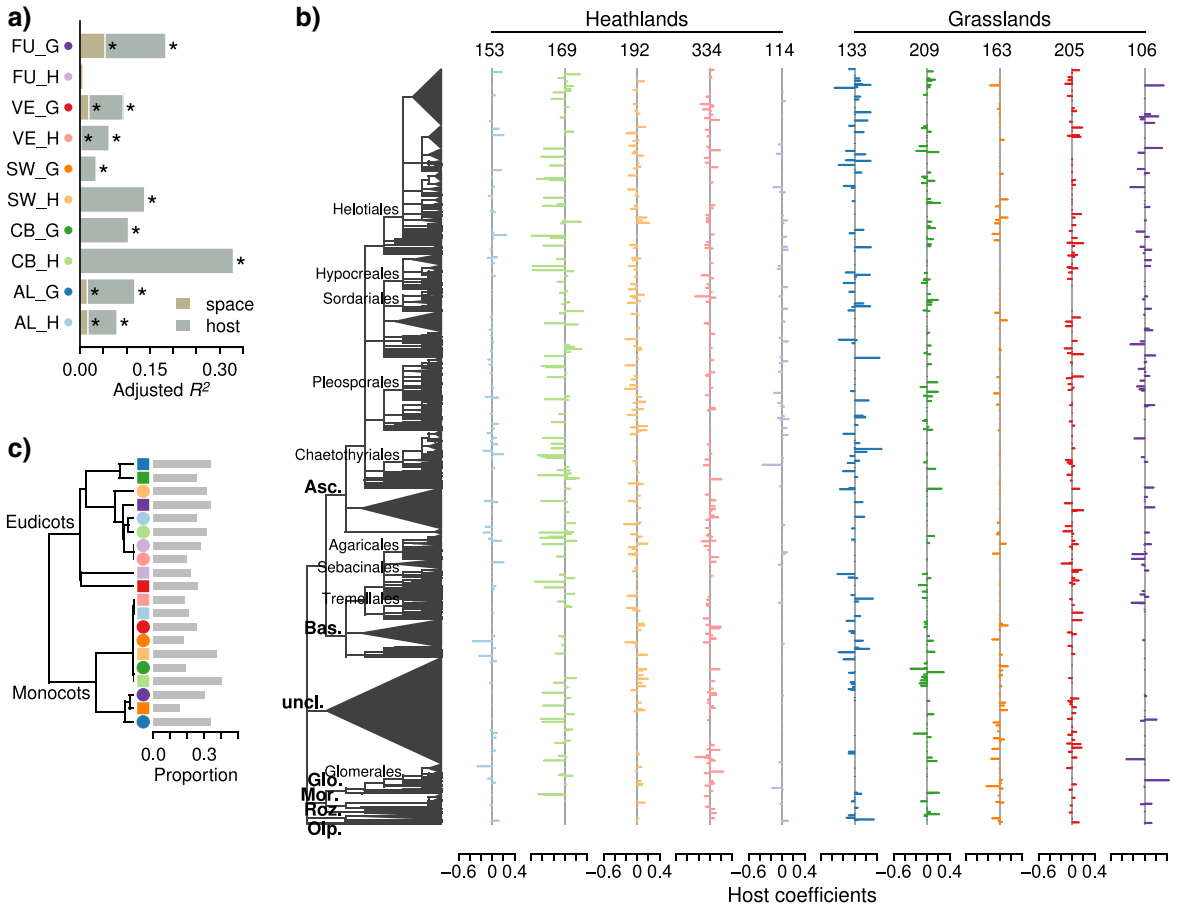

FIG. 6. Host preferences by root-colonizing fungi. (a) Effects of spatial distribution and host identity on whole fungal community structures at each sampling site, based on distance-based redundancy analyses (db-RDA). The bars show the proportion of variance explained (adjusted R^2) by either selected principal coordinates of neighborhood matrix (PCNM) vectors representing spatial structures in the data, or by host species. Asterisks indicate that the amount of variation explained is different to that explained by a random model at $P < 0.01$. (b) Multispecies general linear model (GLM) coefficients indicating correlations between individual OTUs and either of the two hosts collected at each sampling site. Coefficients with positive or negative values substantially contributed to differences between hosts, as assessed by model selection using LASSO penalties; coefficients that did not contribute to such variation were set to zero. In all cases, except for sites SW_G and FU_H, negative values indicate association with a monocot host, and positive values with a eudicot host. At SW_G, two monocots were sampled, with negative values showing association with *Deschampsia flexuosa*, and positive values with *Trichophorum cespitosum*. In FU_H, two eudicots were collected, with negative and positive values indicating associations with *Betula nana* and *Calluna vulgaris*, respectively. The numbers above bar charts indicate the number of OTUs included in each site's GLM model. The OTUs are sorted vertically according to their phylogenetic affiliation, following the phylogenetic tree on the left. In the tree, the most abundant taxa are indicated, and terminal clades with five or more tips are collapsed into triangles. (c) Proportion of OTUs with positive GLM coefficients for each host plant.

values indicate associations with *Trichophorum cespitosum* (L.) Hartm. or *B. nana*, and negative values with *Deschampsia flexuosa* Trin. or *Calluna vulgaris* Salisb., respectively. All plants in all sites showed significantly associated OTUs that were evenly distributed across fungal phylogeny, without any apparent pattern discriminating eudicots and monocots, nor with a clustering of coefficients by fungal clades. The latter was confirmed by measurements of phylogenetic signal in the host coefficients across fungal phylogeny using Blomberg's K, which yielded values below one ($K = 0.22$–0.35, $P = 0.135$–0.877), indicative of lack of conservatism. Similarly, root colonization by particular mycorrhizal groups was not phylogenetically conserved across plants, as ErM, EcM, and AM fungi were detected in all plant species at similar rates (Appendix S1: Fig. S12, and data online at https://doi.org/10.6084/m9.figshare.12988187). In site CB_H, where the effect of host plant on fungal communities was the highest, we also found the highest absolute coefficient values distributed across fungal taxa, and indicating that strong associations toward the local grass, *Vulpia* sp., are mainly responsible for the differences found between hosts at this site (Fig. 6b). *Vulpia* sp. in CB_H also showed the largest proportion (0.4)

of associated OTUs of all plants, followed by *D. flexuosa* in SW_H (0.38, Fig. 6c). However, no differences in the proportion of positively associated OTUs were found across plant families or habitat types ($F_{5,14} = 0.26$, $P = 0.929$). In Appendix S1: Fig. S13 we illustrated examples of significant associations, and lack thereof, between hosts and OTUs at every site.

A partition of fungal community variances into different deterministic and stochastic ecological processes showed that drift—i.e., random fluctuations in species abundances—was the most important contributor to community assembly (60–88% of variance), followed by dispersal limitation (5–36%; Appendix S1: Fig. S14). However, this assessment failed to detect the contribution of host selection, particularly at CB_H, evident in other analyses. This possibly is the result of the poor phylogenetic signal in the fungal preferences for plant hosts disclosed above, which conflicts with the method's underlying assumption for attributing community variance to deterministic processes: that phylogeny reflects functional traits (Zhou and Ning 2017).

Discussion

Root-associated fungi in heathlands and grasslands assemble into communities that are strongly site specific, driven by environmental selection of species by local climatic and edaphic conditions, but also by a markedly restricted distribution of most fungi. Host plant identity, instead, plays no important role in determining the large-scale occurrence of fungi, and its effects in recruiting specific fungal communities locally are relatively small. Contrarily to what we expected, the two habitat types and the characteristic plants they shelter did not associate with stable, phylogenetically distinct fungal assemblages across a latitudinal gradient imposing major biogeochemical clines. Alternatively, a core set of major fungal lineages was represented everywhere by distinct lower clades—often site-specific OTUs within widespread genera—that apparently are locally adapted. This implies, first, a convergent evolution in phylogenetically distant lineages toward the root-colonizing habit irrespective of the environmental context; and second, that communities formed by distinct species probably are functionally redundant in strategies for habitat colonization and interaction with plant hosts.

Our results are in line with previous studies that highlighted the principal role of spatial distance and climate in shaping the biogeography of soil and root-associated fungi (Talbot et al. 2014, Tedersoo et al. 2014, Coleman-Derr et al. 2016, Glynou et al. 2016, Thiergart et al. 2020), as well as the comparably trivial contribution of host phylogeny (Glynou et al. 2018*b*, Maciá-Vicente et al. 2020*a*, Thiergart et al. 2020). They therefore fit into a popular framework that explains community structure at a given place by the interplay of ecological processes acting at different spatial scales, with dispersal limitation—due to both geographic barriers and species life histories—and climate being first-order determinants of community structure at the broadest scale, and local environmental conditions, niche differentiation, and competition gaining relevance at increasingly smaller scales (Peay et al. 2010, 2016, Adams et al. 2013, Talbot et al. 2014). However, our spatially explicit sampling design, spanning scales from less than one meter to thousands of km, also revealed broad-scale diversity patterns emerging from processes that operated very locally (Levin 1992). Thereby, the pronounced endemism we found cannot be exclusively ascribed to pure dispersal limitation or environmental filtering. The large number of OTUs unique to one site (nearly three-quarters of all OTUs), even in adjacent plots as close as 40 m (in SW), reflects a spatial turnover in communities that is too fast and therefore only captured by our finest-grained measurements. More than half of the site-specific OTUs (2,775 out of 4,888) were in fact unique to individual plant specimens, suggesting that local processes such as biotic interactions, niche partitioning, or ecological drift (Zhou and Ning 2017) are at play in constraining the spread of fungi across neighboring plants, and concomitantly give rise to emergently higher diversities at larger scales. The high rate of small-scale endemism we disclose is remarkably similar to that previously found in North American forest soils (Talbot et al. 2014), which suggests it may be common across natural fungal communities. Such endemism has important implications for upscaling global fungal richness from local measurements, predicting diversity loss linked to habitat degradation and global change, and understanding the role of fungi in ecosystems function.

An important feature of our experimental design is the simultaneous sampling of adjacent heathlands and grasslands across a latitudinal transect, in an attempt to identify widespread fungal groups adapted toward either habitat. The absence of general habitat-specific communities indicates that potential unifying effects of habitat types are overridden by other abiotic, biotic, and/or historical gradients that co-vary with latitude (Hillebrand 2004, Mittelbach et al. 2007). For example, most European heathlands are subject to strong human management, including practices such as grazing by different cattle species, burning, or clearing of vegetation, which probably leave a footprint on the local assemblages of both macro- and microorganisms. The wide array of ecological and historical factors can lead to the formation of various types of heathlands and grasslands (Price 2003), which explains, for example, the lack of distinctive edaphic conditions for each habitat disclosed by our characterization of soil chemistry. Altogether, the disjoint variance between plant and fungal lineages indicated that different factors govern species assembly in both kingdoms. At any rate, the contrasting soil conditions between neighboring sites propitiated a rapid turnover of OTUs across short distances and nearly invariant climates, resulting in a larger contribution than usually reported of edaphic factors at explaining fungal

community variation, relative to climate and spatial distance (Tedersoo et al. 2014; Coleman-Derr et al. 2016; Glynou et al. 2016; Větrovský et al. 2019; Thiergart et al. 2020; but see Glynou et al. 2018*a*). The broad habitat heterogeneity across our survey may have also hampered the detection of widespread fungi with narrow niche breadths. Although fungal dispersal through air and soil is quite limited (Ettema and Wardle 2002, Peay et al. 2010, 2012), many soil and root-associated fungi have been shown to be widespread (Queloz et al. 2011, Cox et al. 2016, Glynou et al. 2017, Maciá-Vicente et al. 2020*b*). In such cases, environmental filtering may become the main driver of the biogeography of species with fastidious habitat preferences, as shown both for fungi (Cox et al. 2016, Glynou et al. 2018*a*) and other microorganisms (Carbonero et al. 2014, Ryšánek et al. 2015) sampled across ecologically similar but spatially distant environments. Therefore, the diversity patterns and relative importance of ecological processes we have reported here must be understood within the peculiarities of our study, as they largely depend on experimental settings such as scale, grain size, and focal habitats and organisms; the same is true, nevertheless, for any such study (Levin 1992).

No major fungal lineages appear to be selected by environmental factors or host phylogeny, suggesting a pervasive lack of specific local adaptations in higher taxa. Thereby, a small subset of widespread, species-rich orders (spearheaded by the Helotiales, Agaricales, Chaetothyriales, Pleosporales, and Hypocreales) dominate throughout our survey irrespective of the extant biotic and abiotic context, as they do in plant roots and soils worldwide (Tedersoo et al. 2014, Cox et al. 2016, Glynou et al. 2018*a*, Toju et al. 2019, Thiergart et al. 2020). Similar patterns of widespread occurrence are evident across less inclusive taxa up to subgeneric ranks, and then marked cross-site differences in community composition are established by distinctive OTUs. This implies that multiple lineages share the physiological traits to colonize diverse habitats and are sufficiently dispersal efficient to reach geographically distant locations. Then, fine-tuned local adaptations occur by selective processes operating rapidly and recently over evolutionary time to differentiate locally distinct populations. This model of local adaptation has been proposed for root endophytic fungi based on differential effects on plant growth by closely related fungi (Kia et al. 2017), and has been described for other microbial groups (Ryšánek et al. 2015). It is further supported by a generalized phylogenetic clustering, mainly involving clumping of related OTUs, which suggests a degree of habitat filtering of communities (Webb 2000). In spite of not hosting specific communities, heathland and grassland habitats seem to impose different pressures on fungal assembly based on contrasting diversity patterns. Heathlands host richer but more phylogenetically clustered assemblages than grasslands, possibly arising from a higher niche heterogeneity (e.g., by co-existing shrubs and grasses with varying degrees of root lignification, compared with grasses and forbs with non-lignified roots prevailing in grasslands) that favors the occurrence of distinct local guilds of fungi, each hosting related lineages adapted to exploit different resources.

It is remarkable that eudicot and monocot hosts that diverged 140–150 million years ago (Ma) (Chaw et al. 2004) do not associate with highly specific assemblages of root-colonizing fungi. The relatively weak and unspecific effects of host phylogeny in recruiting fungi have been shown elsewhere (Glynou et al. 2018*b*, Põlme et al. 2018, Maciá-Vicente et al. 2020*a*, Thiergart et al. 2020), suggesting a generally facultative nature of the root-colonizing habit across fungi (Glynou et al. 2018*a*). This does not mean that plant species do not determine at all the fungal assemblages colonizing their roots. As in previous studies (Wehner et al. 2014, Mommer et al. 2018, Francioli et al. 2020), we found a relationship between community structure and host identity, but it seems more evident at the levels of plant species or genera and less so at higher taxonomic ranks, similar to that recently reported by Tedersoo et al. (2020*a*). In any case, the local effects of plant identity were always small relative to other sources of variation, probably attributable to stochastic processes given the lack of small-scale, deterministic distribution patterns measured by PCNM vectors, and as indicated by the iCAMP analysis. Although differences between plant species appear to be chiefly quantitative (i.e., due to variable fungal abundances, rather than to presence/absence), they could lead to significant impacts on host's performance depending on the qualitative outcome of interactions. Thereby, the differential development of mutualistic or pathogenic associations with a fungus may result in positive or negative competitive relationships between co-existing plant hosts (Fitter 2005, Mommer et al. 2018). This is exemplified in our dataset by the widespread occurrence of mycorrhizal fungi across plant hosts, irrespective of the effective development of mycorrhizas, which indicates that root colonization is necessary, yet not sufficient, for the development of such intimate symbioses. Whereas previous evidence exists about the ability of mycorrhizal fungi to colonize non-receptive roots (Vrålstad 2004, Cosme et al. 2018, Toju and Sato 2018, Tedersoo et al. 2020*b*), this study provides comprehensive support across mycorrhizal guilds of fungi and plants.

Conclusions

Our results show that, whereas communities of root-associated fungi are highly specific locally, they invariably comprise representatives of a phylogenetically diverse array of lineages, and are likely to share a core set of functional traits that drive key ecosystem processes such as decomposition, nutrient cycling, or plant interactions. This implies a functional redundancy across habitats that has been suggested for soil fungi (Talbot et al. 2014), and that is indirectly hinted at here

by the common fungus–root interactions observed microscopically throughout our sampling. Consequently, future studies aimed at elucidating the ecological roles of fungi must increasingly rely upon direct characterizations of functional traits, rather than upon community structure assessments alone. This may involve increased efforts to cultivate yet uncultivated fungi, systematically compiling in a structured way phenotypic and genomic traits from living fungal specimens, and shifting from metabarcoding to metagenomic studies to catalog fungal functions *in situ*.

Acknowledgments

This study was supported by the German Research Foundation (*Deutsche Forschungsgemeinschaft*) under grant MA7171/1-1. We thank regional authorities, as well as personnel from Natural Park Los Alcornocales (Spain), Cabañeros National Park (Spain), Black Forest National Park (Germany), Natuurmonumenten (The Netherlands), and Fulufjället National Park (Sweden) for issuing the sampling permits and for assistance in the field. We also thank Elly Morriën for help in selecting the sites in The Netherlands, Jörn Buse for his critical revision of the manuscript, Meike Piepenbring for support throughout the project, and three anonymous reviewers for their useful feedback on the manuscript.

Literature Cited

Adams, R. I., M. Miletto, J. W. Taylor, and T. D. Bruns. 2013. Dispersal in microbes: fungi in indoor air are dominated by outdoor air and show dispersal limitation at short distances. ISME Journal 7:1262–1273.

Anders, S., and W. Huber. 2010. Differential expression analysis for sequence count data. Genome Biology 11:R106.

Bates, D., M. Mächler, B. Bolker, and S. Walker. 2015. Fitting linear mixed-effects models using LME4. Journal of Statistical Software 67:1–48.

Bender, S. F., C. Wagg, and M. G. A. van der Heijden. 2016. An underground revolution: biodiversity and soil ecological engineering for agricultural sustainability. Trends in Ecology & Evolution 31:440–452.

Blomberg, S. P., T. Garland, and A. R. Ives. 2003. Testing for phylogenetic signal in comparative data: behavioral traits are more labile. Evolution 57:717–745.

Brown, J. H. 1984. On the relationship between abundance and distribution of species. American Naturalist 124:255–279.

Callahan, B. J., P. J. McMurdie, and S. P. Holmes. 2017. Exact sequence variants should replace operational taxonomic units in marker-gene data analysis. ISME Journal 11:2639–2643.

Callahan, B. J., P. J. McMurdie, M. J. Rosen, A. W. Han, A. J. A. Johnson, and S. P. Holmes. 2016. DADA2: High resolution sample inference from Illumina amplicon data. Nature Methods 13:581–583.

Carbonero, F., B. B. Oakley, and K. J. Purdy. 2014. Metabolic flexibility as a major predictor of spatial distribution in microbial communities. PLoS One 9:e85105.

Chaw, S.-M., C.-C. Chang, H.-L. Chen, and W.-H. Li. 2004. Dating the monocot–dicot divergence and the origin of core eudicots using whole chloroplast genomes. Journal of Molecular Evolution 58:424–441.

Cheng, T., C. Xu, L. Lei, C. Li, Y. Zhang, and S. Zhou. 2016. Barcoding the kingdom Plantae: new PCR primers for ITS regions of plants with improved universality and specificity. Molecular Ecology Resources 16:138–149.

Coleman-Derr, D., D. Desgarennes, C. Fonseca-Garcia, S. Gross, S. Clingenpeel, T. Woyke, G. North, A. Visel, L. P. Partida-Martinez, and S. G. Tringe. 2016. Plant compartment and biogeography affect microbiome composition in cultivated and native Agave species. New Phytologist 209:798–811.

Cosme, M., I. Fernández, M. G. A. Van der Heijden, and C. M. J. Pieterse. 2018. Non-mycorrhizal plants: the exceptions that prove the rule. Trends in Plant Science 23:577–587.

Cox, F., K. K. Newsham, R. Bol, J. A. J. Dungait, and C. H. Robinson. 2016. Not poles apart: Antarctic soil fungal communities show similarities to those of the distant Arctic. Ecology Letters 19:528–536.

Cross, H., et al. 2017. Fungal diversity and seasonal succession in ash leaves infected by the invasive ascomycete *Hymenoscyphus fraxineus*. New Phytologist 213:1405–1417.

Desdevises, Y., P. Legendre, L. Azouzi, and S. Morand. 2003. Quantifying phylogenetically structured environmental variation. Evolution 57:2647–2652.

Edgar, R. C. 2010. Search and clustering orders of magnitude faster than BLAST. Bioinformatics 26:2460–2461.

Edgar, R. C. 2018. Accuracy of taxonomy prediction for 16S rRNA and fungal ITS sequences. PeerJ 6:e4652.

Egidi, E., M. Delgado-Baquerizo, J. M. Plett, J. Wang, D. J. Eldridge, R. D. Bardgett, F. T. Maestre, and B. K. Singh. 2019. A few Ascomycota taxa dominate soil fungal communities worldwide. Nature Communications 10:1–9.

Ettema, C. H., and D. A. Wardle. 2002. Spatial soil ecology. Trends in Ecology & Evolution 17:177–183.

Fay, P. A., et al. 2015. Grassland productivity limited by multiple nutrients. Nature Plants 1:1–5.

Fielding, A. F., and P. F. Haworth. 2002. Upland Habitats. Routledge, London, UK; New York, New York, USA.

Fitter, A. H. 2005. Darkness visible: reflections on underground ecology. Journal of Ecology 93:231–243.

Francioli, D., J. van Ruijven, L. Bakker, and L. Mommer. 2020. Drivers of total and pathogenic soil-borne fungal communities in grassland plant species. Fungal Ecology 48:100987.

Fu, L., B. Niu, Z. Zhu, S. Wu, and W. Li. 2012. CD-HIT: accelerated for clustering the next-generation sequencing data. Bioinformatics 28:3150–3152.

Glynou, K., T. Ali, A.-K. Buch, S. Haghi Kia, S. Ploch, X. Xia, A. Çelik, M. Thines, and J. G. Maciá-Vicente. 2016. The local environment determines the assembly of root endophytic fungi at a continental scale. Environmental Microbiology 18:2418–2434.

Glynou, K., T. Ali, S. H. Kia, M. Thines, and J. G. Maciá-Vicente. 2017. Genotypic diversity in root-endophytic fungi reflects efficient dispersal and environmental adaptation. Molecular Ecology 26:4618–4630.

Glynou, K., B. Nam, M. Thines, and J. G. Maciá-Vicente. 2018*a*. Facultative root-colonizing fungi dominate endophytic assemblages in roots of nonmycorrhizal *Microthlaspi* species. New Phytologist 217:1190–1202.

Glynou, K., M. Thines, and J. G. Maciá-Vicente. 2018*b*. Host species identity in annual Brassicaceae has a limited effect on the assembly of root-endophytic fungal communities. Plant Ecology & Diversity 11:569–580.

Hijmans, R. J. 2017. Package'raster'. Geographic Data Analysis and Modeling. R package version 2.8-19. https://cran.r-project.org/web/packages/raster/index.html

Hillebrand, H. 2004. On the generality of the latitudinal diversity gradient. American Naturalist 163:192–211.

Kembel, S. W., P. D. Cowan, M. R. Helmus, W. K. Cornwell, H. Morlon, D. D. Ackerly, S. P. Blomberg, and C. O. Webb. 2010. Picante: R tools for integrating phylogenies and ecology. Bioinformatics 26:1463–1464.

Kia, S. H., K. Glynou, T. Nau, M. Thines, M. Piepenbring, and J. G. Maciá-Vicente. 2017. Influence of phylogenetic conservatism and trait convergence on the interactions between fungal root endophytes and plants. ISME Journal 11:777–790.

Klein, T., R. T. W. Siegwolf, and C. Körner. 2016. Belowground carbon trade among tall trees in a temperate forest. Science 352:342–344.

Kõljalg, U., et al. 2005. UNITE: a database providing web-based methods for the molecular identification of ectomycorrhizal fungi. New Phytologist 166:1063–1068.

Legendre, P., and L. F. J. Legendre. 2012. Numerical ecology. Volume 24, Third Edition. Elsevier, Amsterdam, The Netherlands.

Lekberg, Y., M. Vasar, L. S. Bullington, S.-K. Sepp, P. M. Antunes, R. Bunn, B. G. Larkin, and M. Öpik. 2018. More bang for the buck? Can arbuscular mycorrhizal fungal communities be characterized adequately alongside other fungi using general fungal primers? New Phytologist 220:971–976.

Leopold, D. R. 2016. Ericoid fungal diversity: Challenges and opportunities for mycorrhizal research. Fungal Ecology 24:114–123.

Levin, S. A. 1992. The problem of pattern and scale in ecology: the Robert H. Macarthur award lecture. Ecology 73:1943–1967.

Maciá-Vicente, J. G., B. Nam, and M. Thines. 2020*a*. Root filtering, rather than host identity or age, determines the composition of root-associated fungi and oomycetes in three naturally co-occurring Brassicaceae. Soil Biology and Biochemistry 146:107806.

Maciá-Vicente, J. G., M. Piepenbring, and O. Koukol. 2020*b*. Brassicaceous roots as an unexpected diversity hot-spot of helotialean endophytes. IMA Fungus 11:16.

Maciá-Vicente, J. G., and F. Popa. 2021. Online Supporting Information for Maciá-Vicente and Popa (2021) Ecological Monographs. Figshare, online resource. https://doi.org/10.6084/m9.figshare.12988187.v1

McMurdie, P. J., and S. Holmes. 2014. Waste not, want not: why rarefying microbiome data is inadmissible. PLOS Computational Biology 10:e1003531.

Mittelbach, G. G., et al. 2007. Evolution and the latitudinal diversity gradient: speciation, extinction and biogeography. Ecology Letters 10:315–331.

Mommer, L., et al. 2018. Lost in diversity: the interactions between soil-borne fungi, biodiversity and plant productivity. New Phytologist 218:542–553.

Nguyen, N. H., Z. Song, S. T. Bates, S. Branco, L. Tedersoo, J. Menke, J. S. Schilling, and P. G. Kennedy. 2016. FUNGuild: An open annotation tool for parsing fungal community datasets by ecological guild. Fungal Ecology 20:241–248.

Ning, D., M. Yuan, L. Wu, Y. Zhang, X. Guo, X. Zhou, Y. Yang, A. P. Arkin, M. K. Firestone, and J. Zhou. 2020. A quantitative framework reveals ecological drivers of grassland microbial community assembly in response to warming. Nature Communications 11:4717.

Oksanen, J., F. G. Blanchet, M. Friendly, R. Kindt, P. Legendre, D. McGlinn, P. R. Minchin, R. B. O'Hara, G. L. Simpson, P. Solymos, M. H. H. Stevens, E. Szoecs, and H. Wagner. 2019. vegan: Community Ecology Package. https://cran.r-project.org/web/packages/vegan/index.html

Ooms, J., and S. Chamberlain. 2018. phylocomr: Interface to "Phylocom." https://cran.r-project.org/web/packages/phylocomr/index.html

Pauvert, C., M. Buée, V. Laval, V. Edel-Hermann, L. Fauchery, A. Gautier, I. Lesur, J. Vallance, and C. Vacher. 2019. Bioinformatics matters: The accuracy of plant and soil fungal community data is highly dependent on the metabarcoding pipeline. Fungal Ecology 41:23–33.

Peay, K. G., M. I. Bidartondo, and A. Elizabeth Arnold. 2010. Not every fungus is everywhere: scaling to the biogeography of fungal–plant interactions across roots, shoots and ecosystems. New Phytologist 185:878–882.

Peay, K. G., P. G. Kennedy, and J. M. Talbot. 2016. Dimensions of biodiversity in the Earth mycobiome. Nature Reviews Microbiology 14:434–447.

Peay, K. G., M. G. Schubert, N. H. Nguyen, and T. D. Bruns. 2012. Measuring ectomycorrhizal fungal dispersal: macroecological patterns driven by microscopic propagules. Molecular Ecology 21:4122–4136.

Põlme, S., M. Bahram, H. Jacquemyn, P. Kennedy, P. Kohout, M. Moora, J. Oja, M. Öpik, L. Pecoraro, and L. Tedersoo. 2018. Host preference and network properties in biotrophic plant–fungal associations. New Phytologist 217:1230–1239.

Price, E. A. C. 2003. Lowland grassland and heathland habitats. Psychology Press, London, UK; New York, New York, USA.

Queloz, V., T. N. Sieber, O. Holdenrieder, B. A. McDonald, and C. R. Grünig. 2011. No biogeographical pattern for a root-associated fungal species complex. Global Ecology and Biogeography 20:160–169.

R Core Team. 2020. R: a language and environment for statistical computing. R Foundation for Statistical Computing, Vienna, Austria.

Read, D. J., J. R. Leake, and J. Perez-Moreno. 2004. Mycorrhizal fungi as drivers of ecosystem processes in heathland and boreal forest biomes. Canadian Journal of Botany 82:1243–1263.

Revell, L. J. 2012. phytools: An R package for phylogenetic comparative biology (and other things). Methods in Ecology and Evolution 3:217–223.

Ryšánek, D., K. Hrčková, and P. Škaloud. 2015. Global ubiquity and local endemism of free-living terrestrial protists: phylogeographic assessment of the streptophyte alga *Klebsormidium*. Environmental Microbiology 17:689–698.

Schloss, P. D., et al. 2009. Introducing mothur: open-source, platform-independent, community-supported software for describing and comparing microbial communities. Applied and Environmental Microbiology 75:7537–7541.

Smith, D. P., and K. G. Peay. 2014. Sequence depth, not PCR replication, improves ecological inference from next generation DNA sequencing. PLoS One 9:e90234.

Smith, S. E., and D. J. Read. 1997. Mycorrhizal symbiosis. Second edition. Academic Press, New York, New York, USA; London, UK; Burlington, Vermont, USA; San Diego, California, USA.

Talbot, J. M., et al. 2014. Endemism and functional convergence across the North American soil mycobiome. Proceedings of the National Academy of Sciences of the United States of America. 111:6341–6346.

Tedersoo, L., et al. 2014. Global diversity and geography of soil fungi. Science 346:1256688.

Tedersoo, L., et al. 2020*a*. Regional-scale in-depth analysis of soil fungal diversity reveals strong pH and plant species effects in Northern Europe. Frontiers in Microbiology 11:1953.

Tedersoo, L., M. Bahram, and M. Zobel. 2020*b*. How mycorrhizal associations drive plant population and community biology. Science 367:eaba1223.

Tedersoo, L., S. Sánchez-Ramírez, U. Kõljalg, M. Bahram, M. Döring, D. Schigel, T. May, M. Ryberg, and K. Abarenkov. 2018. High-level classification of the fungi and a tool for evolutionary ecological analyses. Fungal Diversity 90:135–159.

Terrer, C., S. Vicca, B. A. Hungate, R. P. Phillips, and I. C. Prentice. 2016. Mycorrhizal association as a primary control of the CO_2 fertilization effect. Science 353:72–74.

Thiergart, T., et al. 2020. Root microbiota assembly and adaptive differentiation among European *Arabidopsis* populations. Nature Ecology & Evolution 4:122–131.

Toju, H., H. Kurokawa, and T. Kenta. 2019. Factors influencing leaf- and root-associated communities of bacteria and fungi across 33 plant orders in a grassland. Frontiers in Microbiology 10:241.

Toju, H., and H. Sato. 2018. Root-associated fungi shared between arbuscular mycorrhizal and ectomycorrhizal conifers in a temperate forest. Frontiers in Microbiology 9:433.

Van der Heijden, M. G., J. N. Klironomos, M. Ursic, P. Moutoglis, R. Streitwolf-Engel, T. Boller, A. Wiemken, and I. R. Sanders. 1998. Mycorrhizal fungal diversity determines plant biodiversity, ecosystem variability and productivity. Nature 396:69.

van der Heijden, M. G. A., F. M. Martin, M.-A. Selosse, and I. R. Sanders. 2015. Mycorrhizal ecology and evolution: the past, the present, and the future. New Phytologist 205:1406–1423.

van Ruijven, J., E. Ampt, D. Francioli, and L. Mommer. 2020. Do soil-borne fungal pathogens mediate plant diversity-productivity relationships? Evidence and future opportunities. Journal of Ecology 108:1810–1821.

Větrovský, T., et al. 2019. A meta-analysis of global fungal distribution reveals climate-driven patterns. Nature Communications 10:5142.

Vohník, M., J. J. Sadowsky, P. Kohout, Z. Lhotáková, R. Nestby, and M. Kolařík. 2012. Novel root-fungus symbiosis in Ericaceae: sheathed ericoid mycorrhiza formed by a hitherto undescribed basidiomycete with affinities to Trechisporales. PLoS One 7:e39524.

Vrålstad, T. 2004. Are ericoid and ectomycorrhizal fungi part of a common guild? New Phytologist 164:7–10.

Wang, Q., G. M. Garrity, J. M. Tiedje, and J. R. Cole. 2007. Naïve bayesian classifier for rapid assignment of rRNA sequences into the new bacterial taxonomy. Applied and Environmental Microbiology 73:5261–5267.

Wang, Y., U. Naumann, S. T. Wright, and D. I. Warton. 2012. mvabund – An R package for model-based analysis of multivariate abundance data. Methods in Ecology and Evolution 3:471–474.

Warton, D. I., F. G. Blanchet, R. B. O'Hara, O. Ovaskainen, S. Taskinen, S. C. Walker, and F. K. C. Hui. 2015. So many variables: joint modeling in community ecology. Trends in Ecology & Evolution 30:766–779.

Webb, C. O. 2000. Exploring the phylogenetic structure of ecological communities: an example for rain forest trees. American Naturalist 156:145–155.

Webb, C. O., D. D. Ackerly, M. A. McPeek, and M. J. Donoghue. 2002. Phylogenies and community ecology. Annual Review of Ecology and Systematics 33:475–505.

Wehner, J., J. R. Powell, L. A. H. Muller, T. Caruso, S. D. Veresoglou, S. Hempel, and M. C. Rillig. 2014. Determinants of root-associated fungal communities within Asteraceae in a semi-arid grassland. Journal of Ecology 102:425–436.

White, T. J., T. Bruns, S. Lee, and J. Taylor. 1990. Amplification and direct sequencing of fungal ribosomal RNA genes for phylogenetics. Pages 315–322 *in* PCR protocols: a guide to methods and applications. Academic Press, San Diego, California, USA.

Zanne, A. E., et al. 2014. Three keys to the radiation of angiosperms into freezing environments. Nature 506:89–92.

Zhou, J., and D. Ning. 2017. Stochastic community assembly: does it matter in microbial ecology? Microbiology and Molecular Biology Reviews 81:e00002–17.

Supporting Information

Additional supporting information may be found online at: http://onlinelibrary.wiley.com/doi/10.1002/ecm.1489/full

Open Research

The Illumina MiSeq sequence data generated in this study are deposited in the NCBI Sequence Read Archive under BioProject number PRJNA640064 at https://www.ncbi.nlm.nih.gov/bioproject/?term=PRJNA640064. The ITS sequences used for the identification of host plants are deposited in NCBI GenBank under accession nos. MT376778–MT376821. All the raw data and code (Maciá-Vicente and Popa 2021) used for the analyses are available in Figshare: https://doi.org/10.6084/m9.figshare.12988187.